Restoration of scanning probe microscope images *

Gopal Sarma Pingali and Ramesh Jain
Computer Science and Engineering
The University of Michigan
Ann Arbor, MI 48109
email: pingali@caen.engin.umich.edu

Abstract

Scanning probe microscopy (SXM), which includes techniques such as scanning tunneling microscopy (STM) and scanning force microscopy (SFM), is becoming popular for 3D metrology in the semiconductor industry and for high resolution 3D imaging of surfaces in Materials Science and Biology. We present imaging models for SXM that take into account the effect of probe geometry on topographic images produced by SXM in "contact" and "non-contact" modes. We formulate methods for restoring an SXM image to obtain the original surface. Criteria for determining certainty of restoration are developed. It is shown that the methods devloped can be expressed in terms of gray scale morphological operators. The efficacy of the approach is demonstrated by applying it to synthetic and real data.

1 Introduction

Scanning probe microscopy (SXM or SPM) is becoming increasingly popular for analyzing surface structure at the atomic level. This form of microscopy started with the invention of the scanning tunneling microscope (STM) by Gerd Binnig and Heinrich Rohrer [1] who won the Nobel Prize in Physics in 1986 for their invention. Since then, several variants of scanning tunneling microscopy have been developed which can be grouped under the title "scanning probe microscopy" (SPM) or "scanning 'X' microscopy" (SXM). Some of these variants are [9] atomic force microscopy (AFM), laser force microscopy (LFM), magnetic force microscopy (MFM), scanning thermal microscopy, and scanning ion conductance microscopy (SICM). Figure 1 shows a schematic diagram of an atomic force microscope (AFM). The main components of a scanning probe microscope are:

i) A probe used for scanning.

ii) A scanning system for rastering the probe across the sample surface.

iii) A sensing mechanism for measuring the height of the probe over the sample surface.

iv) A feedback controller that maintains the probe at a constant height above the scanned surface.

v) A display system for visualization of the measured topography of the surface.

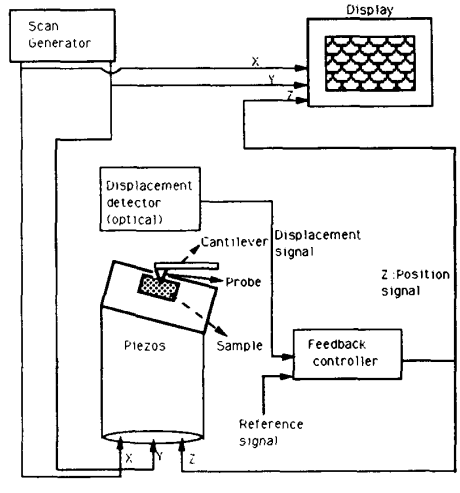

Figure 1: Schematic of an atomic force microscope

Scanning probe microscopes allow the 3D analysis of surface structure with sizes that range down to one angstrom (0.1 nm, about half the diameter of an atom). SXM has great potential for application in several domains such as the semiconductor industry, materials science, and biology. As the probe used for scanning is non-ideal, the image output by SXM is

*This research was supported by the Semiconductor Research Corporation under grant no. 91-MC-085

0-8186-2840-5/92 $03.00 © 1992 IEEE

dependent on the shape and size of the probe. The use and success of SXM strongly depend on methods for ensuring the accuracy of the images produced by SXM.

In this paper, we derive models of the effects of the probe shape geometry on topographic images produced by SXM. It is shown that the imaging process can be modeled by mathematical morphological operations. Constraints imposed by the imaging process are stated and methods for recovering true surface from an image are derived based on these constraints. It is shown that recovery methods can also be expressed in terms of morphological operations. The constraints imposed by the imaging process are also used to derive conditions for certainty of recovery. We derive these methods both for images scanned in a "contact mode" and those scanned in a "non-contact mode". The results we derive are valid for arbitrary probe shapes. The methods derived in this paper can be used to recover a surface scanned by a scanning probe microscope, given the shape of the probe used for scanning, and for visualizing the scanning and recovery of surfaces by different probe shapes.

Section 2 reviews the previous work done on restoration of SXM images. Section 3 presents our model of the imaging process for both contact and non-contact modes. Section 4 presents our methods for surface recovery and for determining the certainty map of the recovery process for both contact and non-contact modes of imaging. Section 5 gives experimental results and section 6 presents conclusions.

2 Related Work

Stoll[8] developed a Wiener filter based approach for restoration that takes into account the significant noise sources in the imaging process and blurring due to the finite size of the probe tip. This approach works only with weakly corrugated samples and is not valid when the sample has high or steep features. Chicon *et al*[2] developed a geometry based algorithm for surface reconstruction in STM. However, their algorithm is severely limited by the assumption of a spherical probe tip that rarely holds in practice.

Gallarda and Jain [3] developed a model of the imaging process in SXM. They propose that the interactions of probe and surface geometries can be modeled in terms of morphological operations. However, they do not rigorously derive their models and the models they propose are valid only under restrictive assumptions about the probe shape. Here, we state the constraints imposed by the imaging process and derive expressions for modeling the imaging process and for restoring SXM images. These expressions are equivalent to those given by us in [6, 7]. We give rigorous derivations of these expressions and show how they can be expressed in terms of gray scale mathematical morphology. The expressions in [3] are special cases of the more general expressions that we derive.

Keller [5] derived a local nonlinear transform called the Legendre Transform for reconstruction of SXM images distorted by the geometry of a non-ideal probe. However, the class of probes for which the method works is limited. The Legendre transform method fails when the probe has the same slope at more than one point. The method has problems when there are discontinuities in the image surface, as it requires computation of derivatives of the image surface at every point. The approach does not handle cases involving multiple points of contact. Finally, as the inverse Legendre Transform could be a many to one mapping , the method often leaves "holes" in the recovered surface.

3 An imaging model for scanning probe microscopy

We make certain assumptions in modeling the imaging process for topographic imaging in SXM. The assumptions are:

- The surface that is being scanned can be represented as a single-valued function $S(x, y)$ with a finite domain denoted D_S.
- The probe that is used for scanning can be represented as a single-valued function $P(x, y)$ with a finite domain P_S.
- During the scanning process, the probe is rastered across the surface of interest and the image output gives the height of a fixed point on the probe. Without loss of generality, the monitored point on the probe can be assumed to be $P(0, 0)$ with a height of 0 as seen in figure 2. That is,

$$P(0, 0) = 0 \tag{1}$$

- In contact mode imaging, each image point $I(x, y)$ corresponds to the height of the monitored point on the probe, when the probe is aligned to (x, y) and the probe just touches the surface S.
- In non-contact mode imaging, each image point $I(x, y)$ corresponds to the height of the monitored point on the probe when the probe is aligned to

(x, y) and the probe is at a specified distance 'd' above the actual surface.

- Non-local effects may be ignored. By this we mean that only the minimum probe-sample distance determines the physical effect (such as tunneling current) that is monitored in scanning probe microscopy and that points on the probe that are at even slightly greater distances do not have any effect. This assumption may be violated in atomic-scale imaging but may be valid for micron and sub-micron scale imaging.

Notice that we allow for arbitrary probe shapes and only assume that there is some point on the probe whose height is monitored during the scanning process. We make no assumptions regarding what the position of this point should be relative to the domain of the probe and can, therefore, allow for asymmetric probes.

3.1 Contact mode Imaging

In this section, we derive a model for contact mode imaging and express it in the convenient notation of mathematical morphology.

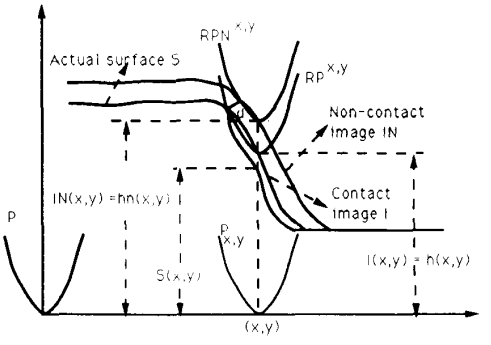

Figure 2: Imaging schematic and labeling conventions

Now, as the probe is rastered across the surface, if it is aligned to coordinates (x_o, y_o), the probe shape function can be given by $P(x-x_o, y-y_o)$. This can be represented as $P_{x_o,y_o}(x, y)$ where we use the notation

$$f_{a,b}(x, y) = f(x - a, y - b) \tag{2}$$

to denote the translation of function f by (a, b). When the probe is aligned to some point (x, y), it is raised by some height $h(x, y)$ so that the corresponding raised probe shape $RP^{x,y}$ (see figure 2) is given by

$$RP^{x,y}(p, q) = P_{x,y}(p, q) + h(x, y) \tag{3}$$

The image height corresponding to coordinates (x, y) is given by

$$I(x, y) = RP^{x,y}(x, y) = P_{x,y}(x, y) + h(x, y) \tag{4}$$

But, we have

$$P_{x,y}(x, y) = P(x - x, y - y) = P(0, 0) = 0 \tag{5}$$

Therefore,

$$I(x, y) = h(x, y) \tag{6}$$

The question is to determine $h(x, y)$. For this, we use constraints imposed by the imaging process. These constraints follow from the assumptions about the imaging process that were stated earlier.

Constraint 1: In contact mode, corresponding to every image point, the probe touches the actual surface atleast at one point.

Hence, we have

$\forall(x, y) \epsilon D_I$, $\exists(x_a, y_a) \epsilon D_S$ such that

$$RP^{x,y}(x_a, y_a) = S(x_a, y_a) \tag{7}$$

where we use the notation D_f to denote the domain of function f.

Using equations 3, 6 and 7, we have

$\forall(x, y) \epsilon D_I$, $\exists(x_a, y_a) \epsilon D_S$ such that

$$I(x, y) = S(x_a, y_a) - P_{x,y}(x_a, y_a) \tag{8}$$

Another constraint imposed by the imaging process may be stated as follows.

Constraint 2: Corresponding to every image point in a contact mode image, the raised probe height is always greater than or equal to the corresponding surface height. This can be expressed as

$\forall(x, y), (x_1, y_1) \epsilon D_S$

$$RP^{x,y}(x_1, y_1) \geq S(x_1, y_1) \tag{9}$$

Or, using equations 3 and 6,

$\forall(x, y), (x_1, y_1) \epsilon D_S$

$$I(x, y) \geq S(x_1, y_1) - P_{x,y}(x_1, y_1) \tag{10}$$

Or,

$\forall(x, y) \epsilon D_S$

$$I(x, y) \geq max_{(x_1,y_1)\epsilon D_S}(S(x_1, y_1) - P_{x,y}(x_1, y_1)) \tag{11}$$

From equations 8 and 11, we have

$$I(x, y) = max_{(x_1,y_1)\epsilon D_S}(S(x_1, y_1) - P_{x,y}(x_1, y_1)) \tag{12}$$

This equation defines a model of the imaging process in contact-mode imaging. We now try to express

this equation in terms of gray scale mathematical morphological operators. The morphological operation of gray scale Minkowski addition or gray scale dilation of two functions f and g is defined as [4]

$$f \oplus g = max_{(x,y)\epsilon D_f}(f(x,y) + g_{x,y}) \quad (13)$$

Using the notation $f^\wedge$ to denote the reflection of function f about the origin, i.e.,

$$f^\wedge(x,y) = -f(-x,-y) \quad (14)$$

we have the following relation between functios P and $P^\wedge$

$$\begin{aligned} P_{x,y}(x_1,y_1) &= P(x_1 - x, y_1 - y) \\ &= -P^\wedge(x - x_1, y - y_1) \\ &= -P^\wedge{}_{x_1,y_1}(x,y) \end{aligned} \quad (15)$$

From equations 12, 14, 15 and 13 we have

$$\begin{aligned} I(x,y) &= max_{(x_1,y_1)\epsilon D_S}(S(x_1,y_1) + P^\wedge{}_{x_1,y_1}(x,y)) \\ &= [S \oplus P^\wedge](x,y) \end{aligned} \quad (16)$$

Equation 16 gives a model of the imaging process in contact mode as the morphological dilation of the surface shape with the reflection of the probe shape about the origin. Note that this model differs from that given in [3] which does not consider the necessity of reflection of the probe shape about the origin before performing the dilation.

3.2 Imaging in a non-contact mode

In Section 3.1, we considered the case when the probe scans a surface in a contact mode. However, in many versions of scanning probe microscopy, the probe maintains a non-negligible constant distance 'd' from the surface being scanned. As in the case of non-contact mode imaging, we use constraints imposed by the imaging process to derive a model of the imaging process.

When the probe is aligned to some point (x,y) while scanning in non-contact mode, it is raised by some height $hn(x,y)$ so that the corresponding raised probe shape $RPN^{x,y}$ (see figure 2) is given by

$$RPN^{x,y}(p,q) = P_{x,y}(p,q) + hn(x,y) \quad (17)$$

Now, the image height corresponding to coordinates (x,y) is given by

$$IN(x,y) = RPN^{x,y}(x,y) = P_{x,y}(x,y) + hn(x,y) \quad (18)$$

But, we have

$$P_{x,y}(x,y) = P(x - x, y - y) = P(0,0) = 0 \quad (19)$$

Therefore,

$$IN(x,y) = hn(x,y) \quad (20)$$

The question is to determine $hn(x,y)$. For this, we use constraints imposed by the imaging process which follow from the assumptions stated earlier.

Constraint 3: In non-contact mode, corresponding to every image point, atleast one point on the probe is exactly at a distance 'd' from atleast one point on the actual surface.

Hence, we have

$\forall(x,y)\epsilon D_{IN}$, $\exists(x_a,y_a),(x_b,y_b)\epsilon D_S$ such that

$$RPN^{x,y}(x_a,y_a) = S(x_b,y_b) + g^d(x_b - x_a, y_b - y_a) \quad (21)$$

where the function g^d gives the height at coordinates (x,y) of a hemisphere of radius d centered at the origin and is defined as

$\forall(x,y) : x^2 + y^2 \leq d$

$$g^d(x,y) = \sqrt{d^2 - x^2 - y^2} \quad (22)$$

Equation 21 may be rewritten as

$\forall(x,y)\epsilon D_{IN}$, $\exists(x_a,y_a),(x_b,y_b)\epsilon D_S$ such that

$$RPN^{x,y}(x_a,y_a) = S(x_b,y_b) + g^d{}_{x_b,y_b}(x_a,y_a) \quad (23)$$

where we have made use of the fact $g^d(x,y) = g^d(-x,-y)$. Using equations 17, 20, and 23,we have

$\forall(x,y)\epsilon D_{IN}$, $\exists(x_a,y_a),(x_b,y_b)\epsilon D_S$ such that

$$IN(x,y) = S(x_b,y_b) + g^d{}_{x_b,y_b}(x_a,y_a) - P_{x,y}(x_a,y_a) \quad (24)$$

which may be rewritten as

$\forall(x,y)\epsilon D_{IN}$, $\exists(x_a,y_a),(x_b,y_b)\epsilon D_S$ such that

$$IN(x,y) = S(x_b,y_b) + g^d{}_{x_b,y_b}(x_a,y_a) + P^\wedge{}_{x_a,y_a}(x,y) \quad (25)$$

where $P^\wedge$ is defined as in equation 14.

Another constraint imposed by the imaging process in non-contact mode is as follows.

Constraint 4: Corresponding to every point in a non-contact mode image, the raised probe height is always at a distance greater than or equal to d from actual surface.

This can be expressed as

$\forall(x,y),(x_1,y_1),(x_2,y_2)\epsilon D_S$

$$RPN^{x,y}(x_1,y_1) \geq S(x_2,y_2) + g^d(x_2 - x_1, y_2 - y_1) \quad (26)$$

Or, using equations 17 and 20
$\forall(x,y),(x_1,y_1),(x_2,y_2)\epsilon D_S$

$$IN(x,y) \geq S(x_2,y_2)+g^d(x_2-x_1,y_2-y_1)-P_{x,y}(x_1,y_1) \quad (27)$$

Or, using the notation given in equations 2 and 14
$\forall(x,y),(x_1,y_1),(x_2,y_2)\epsilon D_S$

$$IN(x,y) \geq S(x_2,y_2) + g^d{}_{x_2,y_2}(x_1,y_1) + P^\wedge{}_{x_1,y_1}(x,y) \quad (28)$$

Or,
$\forall(x,y)\epsilon D_S$

$$IN(x,y) \geq max_{(x_1,y_1),(x_2,y_2)\epsilon D_S}(S(x_2,y_2) + g^d{}_{x_2,y_2}(x_1,y_1) + P^\wedge{}_{x_1,y_1}(x,y)) \quad (29)$$

From equations 25 and 29, we have

$$IN(x,y) = max_{(x_1,y_1),(x_2,y_2)\epsilon D_S}(S(x_2,y_2) + g^d{}_{x_2,y_2}(x_1,y_1) + P^\wedge{}_{x_1,y_1}(x,y)) \quad (30)$$

This equation defines a model of the imaging process in non-contact mode imaging. In terms of gray-scale morphologicval dilation, this equation can be written as

$$\begin{aligned} IN(x,y) &= [[S \oplus g] \oplus P^\wedge](x,y) \\ &= [S \oplus g \oplus P^\wedge](x,y) \end{aligned} \quad (31)$$

where we have used the associativity property of morphological dilation.

Therefore, in the non contact-mode the imaging process can be modeled as a two step process. In the first step, the original surface is dilated with a positive hemisphere of radius d centered at the origin. In the second step the result of the first step is dilated with the reflection of the probe shape about the origin. The result of the first step in this two-step process can be considered as the surface resulting from a non-contact mode scan at a distance 'd' by an ideal (single-point) probe.

4 Surface recovery

We now consider the recovery of the original surface given the imaged surface, the probe kernel representing the shape of the probe used in imaging, and in the case of non-contact mode imaging, the distance that is maintained between the surface and the probe.

4.1 Surface recovery in contact mode

Surface recovery can be based on the constraints imposed by the imaging process. Two such constraints for contact mode imaging were stated in section 3.1. One of these constraints is given by equation 10 which can be rewritten as
$\forall(x,y),(x_1,y_1)\epsilon D_I$

$$S(x,y) \leq P_{x_1,y_1}(x,y) + I(x_1,y_1) \quad (32)$$

Or,
$\forall(x,y)\epsilon D_I$

$$S(x,y) \leq min_{(x_1,y_1)\epsilon D_I}(I(x_1,y_1) + P_{x_1,y_1}(x,y)) \quad (33)$$

Hence, an estimate R for the surface S can be given as
$\forall(x,y)\epsilon D_I$

$$R(x,y) = min_{(x_1,y_1)\epsilon D_I}(I(x_1,y_1) + P_{x_1,y_1}(x,y)) \quad (34)$$

This equation defines a method for estimating the original surface S, given the contact-mode image I and the shape P of the probe used for scanning. We now try to express this equation in terms of morphological operators. The gray-scale Minkowski subtraction of two functions g and f is defined as [4]

$$g \ominus f = min_{(x,y)\epsilon D_f}(f(x,y) + g_{x,y}) \quad (35)$$

Hence, equation 34 can be rewritten in terms of Minkowski subtraction as

$$R(x,y) = [P \ominus I](x,y) \quad (36)$$

Equation 36 states that an estimate of the original surface can be obtained by performing a Minkowski subtraction on the probe shape with the shape of the image. Note, that this equation is not in terms of morphological erosion. Also, note the order of P and I as the Minkowski subtraction is not commutative. This equation is different from that given in [3].

4.2 Certainty of recovery in contact mode

An important question is whether we can determine where exactly the reconstructed surface obtained using the surface recovery algorithm of section 4.1 is identical to the original surface. For this, we again use the constraints imposed by the imaging process. The constraint given by equation 8 can be rewritten as
$\forall(x,y)\epsilon D_I$, $\exists(x_a,y_a)\epsilon D_S$ such that

$$S(x_a,y_a) = I(x,y) + P_{x,y}(x_a,y_a) \quad (37)$$

From equations 33 and 37 we have
$\forall(x,y)\epsilon D_I$, $\exists(x_a,y_a)\epsilon D_S$ such that

$$S(x_a,y_a) = min_{(x_1,y_1)\epsilon D_I}(I(x_1,y_1) + P_{x_1,y_1}(x_a,y_a)) \quad (38)$$

From equations 38 and 34 we have,
$\forall(x,y)\epsilon D_I$, $\exists(x_a,y_a)\epsilon D_S$ such that

$$S(x_a,y_a) = R(x_a,y_a) \tag{39}$$

and combining this with equation 37 we have
$\forall(x,y)\epsilon D_I$, $\exists(x_a,y_a)\epsilon D_S$ such that

$$I(x,y) = R(x_a,y_a) - P_{x,y}(x_a,y_a)$$
$$and$$
$$S(x_a,y_a) = R(x_a,y_a) \tag{40}$$

Now, for some $(x1,y1)\epsilon D_I$, if there exists only one (x_a,y_a) which satisfies

$$I(x1,y1) = R(x_a,y_a) - P_{x_1,y_1}(x_a,y_a) \tag{41}$$

we have from the constraint imposed by equation 40 that for such (x_a,y_a), $R(x_a,y_a)$ necessarily = $S(x_a,y_a)$. This may be stated as the following necessary condition for equality of recovered and original surfaces:

$\forall(x,y)\epsilon D_R$
$R(x,y) = S(x,y)$
if $\exists(x_1,y_1)\epsilon D_I$ such that
$R(x,y) = I(x_1,y_1) + P_{x_1,y_1}(x,y)$
and $\forall(x_2,y_2)\epsilon D_R and \neq (x,y)$
$R(x_2,y_2) \neq I(x_1,y_1) + P_{x_1,y_1}(x_2,y_2)$

However, this condition is not a sufficient condition. Hence, the points on the recovered surface that are marked as identical to the original surface are definitely so but some points on the recovered surface may not be marked even when they are identical to the original surface.

4.3 Surface recovery in non-contact mode

As in the case of contact mode, we use the constraints imposed by the imaging process to derive a method for surface recovery in the non-contact mode. The constraint given by 27 in section 3.2 can be rewritten as
$\forall(x,y),(x_1,y_1),(x_2,y_2)\epsilon D_{IN}$

$$S(x,y) \leq IN(x_1,y_1) - g^d{}_{x_2,y_2}(x,y) + P_{x_1,y_1}(x_2,y_2) \tag{42}$$

Or,
$\forall(x,y)\epsilon D_{IN}$

$$S(x,y) \leq min_{(x_1,y_1),(x_2,y_2)\epsilon D_{IN}}(IN(x_1,y_1) + q^d{}_{x_2,y_2}(x,y) + P_{x_1,y_1}(x_2,y_2)) \tag{43}$$

where

$$q^d(x,y) = -g^d(x,y) = -\sqrt{d^2 - x^2 - y^2} \tag{44}$$

Hence, an estimate Rn for the surface S scanned in non-contact mode can be given as
$\forall(x,y)\epsilon D_{IN}$

$$Rn(x,y) = min_{(x_1,y_1),(x_2,y_2)\epsilon D_{IN}}(IN(x_1,y_1) + q^d{}_{x_2,y_2}(x,y) + P_{x_1,y_1}(x_2,y_2)) \tag{45}$$

Equation 45 defines a method for estimating the true surface S, given the non-contact mode image I, the probe-sample distance d, and the shape P of the probe used for scanning. In terms of morphological operators this equation may be rewritten as
$\forall(x,y)\epsilon D_{IN}$

$$Rn(x,y) = [q^d \ominus [P \ominus IN]](x,y) \tag{46}$$

Equation 46 states that an estimate of the original surface can be obtained by first performing a Minkowski subtraction on the probe shape with the shape of the image. Minkowski subtraction is then performed on a negative hemisphere of radius d centered at the origin with the shape of the surface resulting from the first step. This two-step recovery procedure corresponds to the two-step model of the imaging process given in section 3.2.

4.4 Certainty of recovery in non-contact mode

Using the constraints stated in section 3.2 and proceeding as in section 4.2 we can derive the following necessary condition for equality of recovered and original surfaces:
$\forall(x,y)\epsilon D_{Rn}$
$Rn(x,y) = S(x,y)$
if $\exists(x_1,y_1),(x_2,y_2)\epsilon D_I$ such that
$Rn(x,y) = IN(x_1,y_1) + q^d{}_{x_2,y_2}(x,y) + P_{x_1,y_1}(x_2,y_2)$
and $\forall(x_3,y_3)\epsilon D_R$ and $(x_3,y_3) \neq (x,y)$
$Rn(x_3,y_3) \neq IN(x_1,y_1) + q^d{}_{x_2,y_2}(x_3,y_3) +$
$P_{x_1,y_1}(x_2,y_2)$

This is a necessary condition that can be used to determine the certainty of a point on the recovered surface. An interesting point to note is that this condition allows multiple points (x_2,y_2) to correspond to a single point (x_1,y_1) as long as these multiple values map to a single (x,y) on the recovered surface.

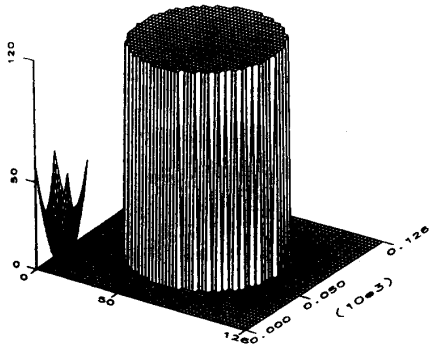

Figure 3: Cylindrical structure and parabaloid probe

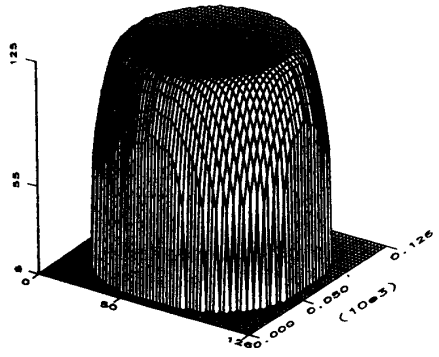

Figure 4: Image from non-contact mode scan

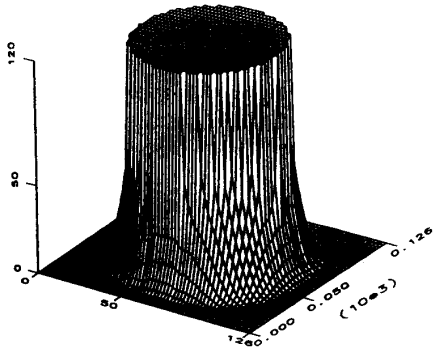

Figure 5: Restored image of cylinder

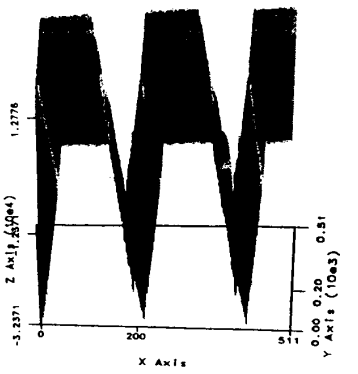

Figure 6: AFM image of V-grooves

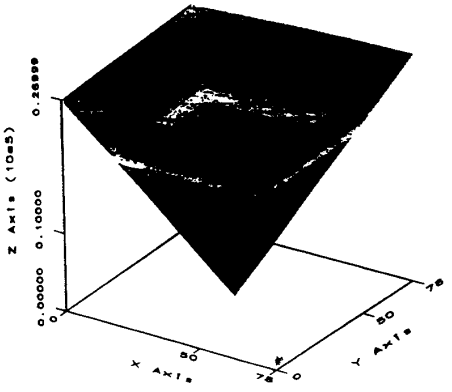

Figure 7: Pyramidal probe used to scan the V-grooves

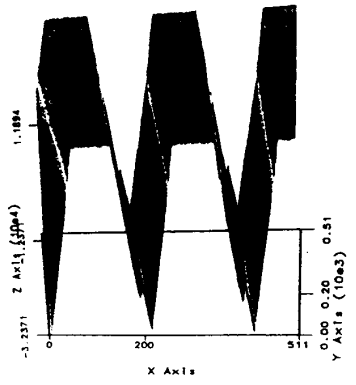

Figure 8: Restored image of V-grooves

5 Experimental Results

We ran several experiments to test the efficacy of our model of the imaging process and our method for surface recovery . Figure 3 shows a synthetic cylindrical structure along with a parabaloid probe used to scan the structure in a non-contact mode at a distance of 5 pixels. Figure 4 shows the image resulting from the scan. Notice that the image is significantly distorted due to the probe shape. Figure 5 shows the final recovered surface using our recovery algorithm. Figure 6 shows a real contact-mode AFM image of V grooves etched in silicon. Figure 7 shows a 3D model of the pyramidal probe that was used for scanning the V-grooves.The model was built from a scanning electron microscope (SEM) image of the probe. Figures 8 shows the surface recovered using our algorithm. Notice that the valleys in the recovered image are wider than those in the original image. The faces in both the original and recovered image are plane as the scanning was done by a pyramidal probe with plane faces. More detailed results are presented in [6].

6 Conclusion

In this paper, we presented models of the imaging process in scanning probe microscopy for both contact and non-contact modes of topographic imaging, taking into account the interaction of the geometries of the probe and the surface. We developed methods for recovering true surface from images scanned in both contact and non-contact modes. We also presented methods for determining where the recovery is exact and where it is uncertain. The methods were tested with several synthetic and real images.

Acknowledgements

We would like to thank L.C. Kong for providing the V-groove structures, John Mansfield for help in using the AFM, Chiao-Fe Shu and Arun Hampapur for stimulating discussions, and one of the reviewers for valuable comments.

References

[1] Binnig, G., Rohrer, H., Gerber, CH., and Weibel, E., *Physical Review Letters*, Vol 49, 57 (1982).

[2] Chicon, R., Ortuno, M., and Abellan, J., "An algorithm for surface reconstruction in scanning tunneling microscopy," *Surface Science*, 181 (1987) pp. 107-111.

[3] Gallarda, H., and Jain, R.,"A computational model of the imaging process in Scanning X Microscopy," Proceedings of Conference on Integrated Circuit Metrology, Inspection and Process Control V, *SPIE Symposium on Microlithography*, San Jose,March 1991.

[4] Giardina, C. R. and Dougherty, E. R., *Morphological Methods in Image and Signal Processing*, Prentice Hall, 1988.

[5] Keller, D.,"Reconstruction of STM and AFM images distorted by finite size tips," *Surface Science*, 253 (1991), pp. 353-364.

[6] Pingali, G.S. and Jain, R., "Imaging Models and Surface Recovery Methods for Scanning Probe Microscopy." *Computer Science and Engineering Technical Report CSE-TR-137-92*, Department of Electrical Engineering and Computer Science, The University of Michigan, Ann Arbor, 1992.

[7] Pingali, G.S. and Jain, R., "Surface Recovery in Scanning Probe Microscopy." SPIE Conference on Machine Vision Applications, Architectures, and Systems Integration,Boston, November 1992.

[8] Stoll, E.P., "Picture processing and three-dimensional visualization of data from scanning tunneling and atomic force microscopy," *IBM Journal of Research and Development*, Vol. 35 No. 1/2 January/March 1991, pp. 67-77.

[9] Wickramasinghe, H.K., "Scanning probe microscopy: Current status and future trends," *Journal of Vacuum Science and Technology*, A 8 (1), Jan/Feb 1990.